HHS Public Access

Author manuscript

Dev Biol. Author manuscript; available in PMC 2016 November 01.

Published in final edited form as:

Dev Biol. 2015 November 1; 407(1): 26–39. doi:10.1016/j.ydbio.2015.08.010.

Gbx2 is essential for maintaining thalamic neuron identity and repressing habenular characters in the developing thalamus

Mallika Chatterjee, **Qiuxia Guo**, and **James Y.H. Li***

Department of Genetics and Genome Sciences, University of Connecticut School of Medicine, 400 Farmington Avenue, Farmington, CT 06030-6403

Abstract

The thalamus and habenula, two important nodes of the forebrain circuitry, are derived from a single developmental compartment, called prosomere 2, in the diencephalon. Habenular and thalamic neurons display distinct molecular identity, neurochemistry, and connectivity. Furthermore, their progenitors exhibit distinctive neurogenic patterns with a marked delay in the onset of neurogenesis in the thalamus. However, the progenitors in prosomere 2 express many common developmental regulators and the mechanism underlying the specification and differentiation of these two populations of neurons remains unknown. *Gbx2*, coding for a homeodomain transcription factor, is initially expressed in thalamic neuronal precursors that have just exited the cell cycle, and its expression is maintained in many mature thalamic neurons in adults. Deletion of *Gbx2* severely disrupts histogenesis of the thalamus and abolishes thalamocortical projections in mice. Here, by using genome-wide transcriptional profiling, we show that *Gbx2* promotes thalamic but inhibits habenular molecular characters. Remarkably, although *Gbx2* is expressed in postmitotic neuronal precursors, deletion of *Gbx2* changes gene expression and cell proliferation in dividing progenitors in the developing thalamus. These defects are partially rescued by the mosaic presence of wild-type cells, demonstrating a cell non-autonomous role of *Gbx2* in regulating the development of thalamic progenitors. Our results suggest that *Gbx2* is essential for the acquisition of the thalamic neuronal identity by repressing habenular identity through a feedback signaling from postmitotic neurons to progenitors.

Keywords

Transcription; cell fate; differentiation; neurogenesis; mouse

INTRODUCTION

The thalamus and habenula are two important nodes of the forebrain circuitry. The habenula, which is a paired midline structure that straddles the posterior and dorsal surface of the

***Corresponding author:** James Y.H. Li, Department of Genetics and Genome Sciences, University of Connecticut School of Medicine, 400 Farmington Avenue, Farmington, CT 06030-6403, jali@uchc.edu.

thalamus, is present in virtually all vertebrates. The habenula receives input from the forebrain limbic system and the basal ganglia through the stria medullaris, and projects to monoaminergic nuclei in the midbrain and hindbrain via the fasciculus retroflexus, also called the habenulopeduncular tract (Lecourtier and Kelly, 2007; Hikosaka et al., 2008). Dysfunction of the habenula has been implicated in psychiatric disorders, such as depression, schizophrenia, and drug-induced psychosis (Hikosaka, 2010). By contrast, the thalamus receives sensory and motor information from the periphery and relays them to the cortex through thalamocortical projections (Jones, 2007). The thalamus is thus considered as the gateway to the cortex and essential for establishing self-consciousness and awareness to one's environment (Sherman and Guillery, 2006). Despite their marked differences in cytoarchitecture and connectivity, thalamic and habenular neurons arise from seemingly homogeneous progenitors. The molecular underpinnings of progenitor differentiation into thalamic and habenular neurons remain elusive.

Based on the pattern of gene expression and axonal tracts, the diencephalon is divided into three developmental compartments called prosomeres (Rubenstein et al., 1994; Puelles and Rubenstein, 2003). Among the three prosomeres (P)1-3 in the diencephalon, P1 gives rise to the pretectum, P2 the thalamus and epithalamus, and P3 the prethalamus. The epithalamus subsequently produces the habenula, pineal gland and choroid plexus. The thalamic progenitor domain can be further divided into rostral and caudal areas: the former gives rise to local GABAergic neuron while the latter to glutamatergic neurons projecting to the cortex (Vue et al., 2007; Jeong et al., 2011). Neurons derived from the caudal thalamus constitute the nuclei complex that is traditionally viewed as the thalamus (Jones, 2007). Significant progress has been made in our understanding of the development of diencephalic prosomeres (Chatterjee and Li, 2012). Extracellular signals, such as Shh (Kiecker and Lumsden, 2004; Scholpp et al., 2006; Jeong et al., 2011) (Vue et al., 2009), FGF(Kataoka and Shimogori, 2008; Martinez-Ferre and Martinez, 2009), and WNT (Zhou et al., 2004; Bluske et al., 2012), which are produced from localized signaling centers, act in concert to pattern the diencephalon. Transcription factors, such as Pax6, Otx2, Fezf2, and Iroquois proteins, also participate in controlling the cell fate of progenitors in different diencephalic prosomeres (Hirata et al., 2006; Puelles et al., 2006; Scholpp et al., 2007; Robertshaw et al., 2013; Chatterjee et al., 2014). We have recently reported the characterization of gene expression in the epithalamus, particularly the habenula in mice and zebrafish (Chatterjee et al., 2014). Interestingly, although postmitotic neuronal precursors for the prospective thalamus and habenula can be readily distinguished by distinct expression patterns of marker genes, P2 progenitors appear remarkably homogenous (Chatterjee et al., 2014). How the P2 domain is partitioned into the future thalamus and epithalamus remains to be determined.

Although it is traditionally believed that cell fate specification occurs in proliferating progenitors, emerging evidence indicate that additional mechanisms determine and/or consolidate cell identity after neural precursors exit the cell cycle (Belliveau and Cepko, 1999; Seuntjens et al., 2009; Hobert, 2011). Experiments in *C. elegance* have identified a class of transcription factors that play an important role in assigning and/or maintaining the identity of postmitotic neurons and are called “terminal selector genes” (Hobert, 2008; Flames and Hobert, 2009). Furthermore, studies in the neocortex and retina have shown that

early-born neurons signal dividing progenitors to ensure the successive generation of cell types (Belliveau and Cepko, 1999; Seuntjens et al., 2009). *Gbx2*, which encodes a homeodomain transcription factor, is expressed in thalamic neuronal precursors that have just exited the cell cycle; its expression is maintained in mature neurons of thalamic nuclei in adult mice and monkeys (Jones and Rubenstein, 2004; Chen et al., 2009). We have previously demonstrated that the *Gbx2* lineage contributes exclusively to thalamic nuclei that project to the cortex (Chen et al., 2009; Li et al., 2012). Deletion of *Gbx2* severely disrupts histogenesis of the thalamus and abolishes thalamocortical projections (Miyashita-Lin et al., 1999; Hevner et al., 2002; Chen et al., 2009; Chatterjee et al., 2012; Li et al., 2012). Interestingly, in the absence of *Gbx2*, thalamic neurons abnormally extend their axons and follow the fasciculus retroflexus tract, reaching the ventral midbrain and hindbrain (Chatterjee et al., 2012). Furthermore, neurons originating from the thalamus aberrantly contribute to the habenula (Chen et al., 2009). These observations raise an intriguing possibility that *Gbx2* determines and/or maintains the cell identity of thalamic neurons.

In this study, we explored the potential role of *Gbx2* in cell fate specification and/or consolidation in the developing thalamus by identifying alterations in the genome-wide transcriptional profile in the thalamus caused by *Gbx2* deletion. We show that *Gbx2* is essential for maintaining the thalamic fate and repressing the habenular development. Using genetic mosaics, we demonstrate that *Gbx2* exerts its function in part by modulating the developmental program in proliferating progenitors of the thalamus through a feedback mechanism from postmitotic neural precursors.

MATERIALS AND METHODS

Mouse and tissue preparation

All animal procedures described herein were approved by the Animal Care Committee at the University of Connecticut School of Medicine. Mice were housed in a facility with a 12-hour light/dark cycle and have free access to food and water. All mouse strains were maintained in a CD1 genetic background (Charles River Lab, Wilmington, MA). Noon of the day on which a vaginal plug was detected was designated as E0.5 in staging of embryos. The generation of knock-in $Gbx2^{creER}$ allele, which expresses both creER and enhanced green fluorescence protein (EGFP) from the *Gbx2* locus, has been described previously (Chen et al., 2009). Embryos carrying the $Gbx2^{creER}$ allele were identified by GFP fluorescence in the spinal cord, cerebellum, and thalamus. The *Gbx2* null ($Gbx2^{-}$) and conditional floxed ($Gbx2^{F}$) alleles were determined by PCR analysis of tail DNA as described previously (Wassarman et al., 1997; Chen et al., 2009).

Taking advantage of the mosaic nature of creER-mediated recombination induced by tamoxifen, we deleted *Gbx2* in a mosaic manner in the thalamus of $Gbx2^{creER/F}$ embryos as described previously (Chen et al., 2009; Chatterjee et al., 2012). As *Gbx2* acts cell autonomously to regulate thalamocortical axon guidance, all mosaic deletion embryos were verified by abnormal thalamic axon trajectories examined by GFP fluorescence that was expressed from the $Gbx2^{cerER}$ locus as described previously (Chatterjee et al., 2012). All reported phenotypes were reproduced in at least three mosaic mutant embryos.

Histochemistry, immunofluorescence, and in situ hybridization

Standard protocols were used for immunohistochemistry (ICH) and *in situ* hybridization (ISH) as described previously (Chatterjee et al., 2012). For bromodeoxyuridine (BrdU) staining, BrdU was dissolved at 0.5 mg/ml in PBS, and injected intraperitoneally into pregnant female mice at 10 μg/g body weights. Embryos were dissected after 7 or 24 hours. Detailed protocols are available on the Li Laboratory website (http://lilab.uchc.edu/protocols/index.html). Primary antibodies used in the study were as follows: rat anti-Ki67 (DAKO); mouse anti-neurofilaments (DSHB hybridoma bank); rabbit anti-pH3 (Merck Millipore); mouse anti-Pou4f1 (Santa Cruz); goat anti-Ox2 (R&D Systems); rabbit anti-GFP (Invitrogen); mouse anti-BrdU (BD Biosciences); rabbit anti-Dbx1 (Vue et al., 2007); rabbit anti-Islr2 (Mandai et al., 2009). Alexa fluorescent secondary antibodies (Invitrogen) were used.

Microarray analysis

The brains of *Gbx2*$^{creER/+}$ or *Gbx2*$^{creER/-}$ embryos at E12.5 were dissected in chilled PBS. Brain slices at 250 μm were produced on a vibratome. Guided by EGFP fluorescence, the thalamus was dissected and quickly frozen for storage before RNA extraction. Total RNA was extracted with TRIzol® (Invitrogen) and purified with RNeasy column (QIAGEN) following manufacturer's instructions. Quality and quantity of the extracted RNA was determined by Bioanalyzer (Agilent Technologies). Hybridizations to the Mouse-6 Expression BeadChip and measurement of hybridization intensities were performed according to the manufacture's procedures (Illumina, San Diego, CA). Summary of raw data was exported from the BeadStudio/GenomeStudio software and processed in the R software environment. Background correction, variance stabilizing transformation and normalization were performed using the background correction, VST and RSN methods implemented in the *lumi* package (Du et al., 2008). To combine the array data from two generations of BeadChip used in our experiments, we resolved the inconsistency of Illumina identifiers through nuID (Du et al., 2008). A total of 18,662, 19,440, and 16,069 genes in the mouse genome were examined by the first, second, and the combined array assays, respectively. Batch effects were corrected using ComBat (Johnson et al., 2007). Differentially expressed genes (DE) were identified using the *limma* package (Ritchie et al., 2015) with a cutoff of adjusted *p* value (false discovery rate-FDR) equal or less than 0.05 and fold change equal or greater than 1.7 (log2 fold change >0.8). All data have been deposited at GEO: GSE71690.

Gene ontology term enrichment analysis was performed using DAVID Bioinformatics Resource (NIH) (Huang da et al., 2009). Gene Set Analysis was performed using the *GSA* package (Subramanian et al., 2005). Gene sets were downloaded from the monthly updated Baderlab genesets (http://baderlab.org/GeneSets) and an epithalamus-enriched gene set was curated based on published expression data (Quina et al., 2009).

Chick electroporation studies

A full-length mouse *Ebf3* cDNA was cloned into a chicken express vector, *pMiwIII*, under the control of the chicken β-actin promoter. Chick electroporation assays were performed as described previously (Olsen et al., 2006). Briefly, 1.0 μg/μl of *pMiwIII-Ebf3* together with 0.5 μg/μl *pMiwIII-EGFP*, which was used to monitor transfected cells, were injected into the

diencephalon of chicken embryos at HH10-12 stage (Hamburger and Hamilton, 1951) and electroporated into the right side of the neural tube with five rectangular electric pulses of 18 V and 50-millisecond intervals. Embryos were dissected at 36 and 55 hours.

RESULTS

Progenitors throughout the P2 compartment express similar developmental regulators

To investigate the developmental programs that establish the thalamic and epithalamic progenitor domains, we examined the expression of several transcription factors that are known as developmental determinants. As described previously (Nakagawa and O'Leary, 2001; Vue et al., 2007), proneural gene *Neurog2* (previously named *Ngn2*) was broadly expressed in the thalamus except for the lateral-most region that is occupied by postmitotic cells at E12.5 (Fig. 1A). *Neurog2* expression domain was also extended to the ventricular zone of the epithalamus (Fig. 1A). *Irx1*, which encodes a transcription factor of the *Iroquois* family, was expressed in the dorsal part of the diencephalon (Cohen et al., 2000). Transcripts of *Irx1* and its paralogous genes *Irx2* and *Irx3* were found throughout the epithalamus, pretectum and prethalamus, as well as the ventricular zone of the thalamus at E12.5 (Fig. 1B and data not shown). It has been shown that basic helix-loops-helix transcription factor Olig3 defines the entire thalamic VZ at E12.5 (Vue et al., 2007). However, *Olig3* transcripts were also detected in the VZ of the epithalamus at E13.5 (Fig. 1C). As described previously (Quina et al., 2009; Chatterjee et al., 2014), robust expression of Dbx1 protein was detected in the epithalamus (Fig. 1D). However, a dorsal-to-ventral gradient of Dbx1 expression was also found in the thalamus at E12.5 (Fig. 1D). Finally, homeodomain transcription factor Otx2, which is essential for the generation of glutamatergic neurons by repressing GABAergic identity in the thalamus (Puelles et al., 2006), was also detected throughout the ventricular zone of the diencephalon (Fig. 1E). Therefore, the progenitor cells of the prospective epithalamus and thalamus share many key developmental regulators.

Gbx2 is essential for repressing Irx genes in postmitotic cells in the thalamus

We and others have demonstrated that *Gbx2* ablation results in profound defects in the histogenesis of the thalamus and axonal outgrowth and guidance to the neocortex (Miyashita-Lin et al., 1999; Hevner et al., 2002; Chen et al., 2009; Chatterjee et al., 2012; Li et al., 2012). To investigate the mechanism by which *Gbx2* controls thalamic development, we analyzed altered gene expression in the thalamus at E11.5, 24 hour after the onset of *Gbx2* induction. To monitor the expression of *Gbx2*, we utilized a $Gbx2^{creER}$ knock-in allele, which contains a *creER-ires-GFP* cassette in the 5' untranslated region of the *Gbx2* gene (Chen et al., 2009). In mouse embryos carrying this allele, creER and GFP are simultaneously expressed in the same spatiotemporal pattern as the endogenous *Gbx2* transcription (Chen et al., 2009). In $Gbx2^{creER/+}$ embryos at E11.5, GFP was detected only in cells immediately underneath the pial surface in the neural tube wall of the thalamus (Fig. 2A). We have previously shown that these GFP+ cells are postmitotic as they express Tubb3 and fail to incorporate BrdU (Chen et al., 2009). *In situ* hybridization (ISH) on immediately adjacent sections showed that *Irx1* transcripts were absent from the presumed *Gbx2*-expressing cells but present in the rest of the thalamus and throughout the epithalamus (Fig.

2A'). Because neurogenesis progresses in a caudal-to-rostral gradient in the developing thalamus (Angevine, 1970; McAllister and Das, 1977), significantly fewer GFP+ cells were detected in the rostral part, compared to the caudal, of the thalamus (Fig. 2B and B'). Interestingly, the negative domain of *Irx1* was hardly detected in the rostral part of the thalamus at E11.5 (Fig. 2B and B'), suggesting that down-regulation of *Irx1* is associated with *Gbx2* induction. In agreement with this notion, *Irx1* transcripts were absent from the postmitotic thalamic cells that express *Gbx2* by E12.5 (Fig. 2E and inset). Importantly, in the absence of *Gbx2*, *Irx1* transcripts were maintained in postmitotic cells in the thalamus at E11.5 and E12.5 (Fig. 2C-F). Three other members of *Iroquois* genes, *Irx2, Irx3,* and *Irx5*, showed a similar expression pattern to that of *Irx1* in wild-type embryos, and they were all ectopically expressed in postmitotic thalamic neuronal precursors in *Gbx2*-KO embryos (Fig. 2G,H, 5B and data not shown). Therefore, *Gbx2* is essential for repressing *Irx* genes in thalamic neural precursors after they exit the cell cycle.

We have recently shown that *Pax6* regulates the partitioning of the epithalamus and thalamus by restricting Shh activity in the ZLI; without Pax6, the thalamus is expanded at the expense of the epithalamus (Chatterjee et al., 2014). Using GFP to follow *Gbx2* transcription in *Pax6*-deficient embryos carrying a $Gbx2^{creER}$ allele, we found that GFP was ectopically expressed in the presumptive epithalamus concomitant with depletion of *Irx1* transcripts (Fig. 2K). By contrast, *Irx1* was expressed throughout the presumptive epithalamus and thalamus in *Pax6* and *Gbx2* double mutant embryos (Fig. 2L), demonstrating that the ectopic expression of *Gbx2* is responsible for the down-regulation of *Irx1*. Collectively, our data show that *Gbx2* plays a crucial role in repressing *Irx1* transcription in the P2 domain.

Gbx2 deletion results in the loss of thalamic markers and ectopic expression of epithalamus-enriched genes

Iroquois transcription factors play important roles in tissue patterning and cell fate specification (Kobayashi et al., 2002; Kiecker and Lumsden, 2004; Robertshaw et al., 2013). To test if the failure to repress multiple *Iroquois* genes might alter the molecular identity of thalamic precursor cells in *Gbx2*-KO mice, we examined how *Gbx2* deletion affected expression of known molecular markers specific for thalamic or habenular neurons. *Rora* and *Id4* are specifically expressed in thalamic neuronal precursors at E12.5 and later stages (Nakagawa and O'Leary, 2003; Zhou et al., 2004)(Fig. 3A,C). In *Gbx2*-KO embryos at E12.5, *Rora* and *Id4* transcripts were depleted in the thalamus (Fig. 3B,D). *Nrp2, Pou4f1,* and *Robo3* are specifically expressed in postmitotic neural precursors in the epithalamus at E12.5 (Chatterjee et al., 2014)(Fig. 3E,G,I'). Notably, these habenular markers were ectopically expressed in the *Gbx2*-deficient thalamus (Fig. 3F,H,J').

We have previously shown that cells originating from the thalamus contribute to epithalamus-derived structures in the absence of *Gbx2*, demonstrating that *Gbx2* is essential for the lineage restriction between the thalamus and epithalamus (Chen et al., 2009). To rule out that the ectopic Pou4f1+ cells in the *Gbx2*-deficient thalamus were caused by abnormal cell movements rather than misregulation of Pou4f1 expression, we genetically marked *Gbx2*-expressing cells by red fluorescence (RFP) in $Gbx2^{creER/-}$; $R26R^{RFP/+}$ embryos by

administrating tamoxifen at E10.5. Pou4f1 immunoreactivity was found in the epithalamus but absent from RFP+ cells in the thalamus of E12.5 *Gbx2*$^{creER/+}$*; R26R*$^{RFP/+}$ embryos that received tamoxifen at E10.5 (Fig. 3I,I'). In *Gbx2*$^{creER/-}$*; R26R*$^{RFP/+}$ embryos, many Pou4f1+ cells were found in the thalamus and the majority of them were colocalized with RFP, demonstrating that they are descendants of the *Gbx2* lineage originating from the thalamus (Fig. 3J,J'). Although some Pou4f1^{+} cells were negative for RFP, these Pou4f1^{+}/RFP^{-} cells were evenly distributed in both dorsal and ventral parts of the thalamus (Fig. 3J), suggesting that these Pou4f1^{+}/RFP^{-} cells may result from incomplete cre-mediated recombination rather than migration from the epithalamus in *Gbx2*-deficient embryos. Collectively, our data show that thalamic neurons fail to express thalamic-specific genes but ectopically express epithalamus-specific markers in the absence of *Gbx2*.

Gbx2 deletion results in global changes of thalamic transcriptome

To gain insight into how *Gbx2* deletion affects development of the thalamus, we performed genome-wide transcriptional profiling of wild-type and *Gbx2*-deficient thalamus at E12.5 by microarray. We chose E12.5 because *Gbx2* mutant phenotypes were clearly detected at this stage and we could obtain sufficient amount tissue and RNA from a single embryo. We dissected the thalamus from brain slices with the guide of GFP fluorescence that demarcated the thalamus in *Gbx2*$^{creER/+}$ (wild type) and *Gbx2*$^{creER/-}$ (Fig. 4A). We also collected diencephalic tissues dorsal and ventral to the GFP+ domain, containing the epithalamus and prethalamus (as well as the rostral thalamus and ZLI), respectively (Fig. 4A). Using a cutoff of global FDR less than 5% and fold change greater than 1.7, we identified 126 differentially expressed (DE) genes, with 76 decreased and 50 increased, in E12.5 thalamus due to *Gbx2* deletion (Tables I and II)(Fig. 4B). Gene ontology and pathway analyses showed that the DE genes are enriched for genes that are involved in brain development, such as neurogenesis, axon projections, and axon guidance (Fig. 4C,D).

To validate the microarray data, we first inspected the expression pattern of the DE genes in gene expression databases such as Mouse Genomic Informatics, Allen Brain Atlas and GenePaint (Visel et al., 2004; Finger et al., 2011; Thompson et al., 2014). Among those DE genes of available expression information, 50% of them (38/76) were found to be either specifically or strongly expressed in the thalamus between E13.5 or E15.5 (Table I). By comparing the thalamus to the neighboring diencephalic tissues (see Methods), we also identified 35 genes that were enriched in the thalamus (FDR≤0.05 and log2FC≥1), and the majority of them were indeed expressed in the thalamus based on data in the expression databases (Table I). Remarkably, 16 of these thalamus-enriched genes (45.7%, Fisher's exact test $p<0.001$) were down regulated in *Gbx2*-deficient thalamus, supporting the notion that *Gbx2* is essential for acquisition or maintenance of the molecular character of the thalamus.

We next performed ISH to confirm that *Gbx2* deletion reduced expression of the presumptive thalamus-specific genes. Out of 18 DE genes that were examined, 16 were notably downregulated in the thalamus of *Gbx2*-KO embryos at E12.5 or E13.5 (Fig. 5A and data not shown; the other two probes gave inconclusive results). Remarkably, *Chst1*, *Hs6st2*, *Glra2*, and *Cd47* were specifically expressed in the thalamus at E12.5, but their transcripts were mostly depleted in *Gbx2*-deficient thalamus (Fig. 5A). Taken together, our expression

studies show that *Gbx2* deletion results in a loss of the molecular signature of the developing thalamus.

Gbx2-deficient thalamus adopts an expression profile of the developing habenula

To investigate the hypothesis that thalamic neurons lacking *Gbx2* assumed a molecular identity similar to that of the habenula, we first inspected the expression pattern of the up-regulated DE genes in the expression databases. Among the 50 up-regulated DE genes, 18 (36.0%) were highly expressed in the epithalamus (Table II). To avoid an arbitrary cut-off in selecting DE genes, we performed Gene Set Analysis (Subramanian et al., 2005) and found that epithalamus-enriched genes compiled from microarray experiments (see details in Methods) were significantly increased in the *Gbx2*-deficient thalamus (enrichment score=0.67, FDR<0.001). Conversely, levels of thalamus-enriched genes were significantly reduced due to *Gbx2* deletion (enrichment score = −2.57, FDR<0.001). ISH confirmed ectopic expression of epithalamus-enriched genes, such as *Lmo3, Irx2, Ebf3, Islr2, Nefm, Cntn2* and *Kif26a*, in the thalamus due to *Gbx2* ablation (Fig. 5B).

Besides Pou4f1, which is specific to the epithalamus (Quina et al., 2009), many other genes that are inhibited by Gbx2, such as *Lmo3, Irx1, Irx2, Ebf3, Islr2*, and *Cntn2*, are expressed in both the epithalamus and pretectum. To investigate the alternative explanation of de-repression of pretectal fate due to *Gbx2* deletion, we identified 12 pretectal markers, including anterior pretectal genes (*Bhlhe22, C1ql2, Cux2, Esrrb, Neurod6, Pax3, Pik3r1*, and *Tfap2d*) and posterior pretectal genes (*Gata3, Six3*, and *Tal1*) using the Allen Developmental Mouse Brain reference atlas (Thompson et al., 2014)(Fig. S1A). Importantly, we have previously shown that the expression of *Bhlhe22* and *Pax3* are unaffected by *Gbx2* deletion (Chen et al., 2009), and none of these pretectal markers were up-regulated due to *Gbx2* deletion (Fig. S1B), suggesting that *Gbx2* deletion does not convert the thalamus to a pretectal fate. Together, our data shows that thalamic neurons adopt molecular features resembling that of the epithalamus in the absence of *Gbx2*.

Gbx2 deletion alters neurogenic progression in the thalamus

Despite the ambiguity of the molecular signatures between the thalamic and epithalamic progenitors, they exhibit distinctive patterns of neurogenic progression with a markedly delayed neurogenesis in the thalamus (Jones, 2007). For example, the habenular nuclei become distinguishable at E14.5, while the neighboring thalamic domain that gives rise to the parataenial, rhomboid, reunions, mediodorsal and anterior nuclei are not discernible until E18.5 in rats (McAllister and Das, 1977). In sharp contrast to the neighboring diencephalic structure, the developing thalamus contains a remarkably large number of basal progenitor cells (Smart, 1972; Wang et al., 2011). Therefore, the prospective thalamus and epithalamus have distinctive developmental programs that control the proliferation and progression of neural progenitors. Indeed, we detected the mRNA and protein of *Nefm* and *Dcx*, whose expression is associated with generation of postmitotic neurons, in the epithalamus at E12.5, at least 24 hours before they were found in the thalamus (Fig. 5B and data not shown). Remarkably, *Nefm* and *Dcx*, which were absent from the wild-type thalamus until E13.5, were expressed in the mantle zone of the thalamus in *Gbx2*-KO embryos at E12.5 (Fig. 5B and Table II), suggesting that inactivation of *Gbx2* accelerates neurogenesis in the thalamus.

Moreover, *Id4*, which codes for a basic helix-loop-helix negative regulator of neurogenesis(Yun et al., 2004; Bedford et al., 2005), was specifically expressed in the wild-type but lost in *Gbx2*-KO thalamus (Fig. 3C,D). Conversely, *Ebf3* was strongly expressed in the epithalamus but its expression was markedly increased in the *Gbx2*-KO thalamus (Fig. 5A). It has been shown that forced expression of *Ebf3* inhibits cell proliferation and increase apoptosis or tumor cells *in vitro* (Garel et al., 1999; Bai et al., 2007). Using a chick electroporation assay, we showed that expression of *Ebf3* indeed promoted neural progenitor cells to exit the cell cycle in the developing thalamus (Fig. S2). These observations suggest that *Gbx2* regulates neurogenic progression in the thalamus, possibly through the control of Id4 and Ebf3. In the absence of *Gbx2*, the neurogenesis is accelerated in the thalamus matching that in the epithalamus.

To investigate if *Gbx2* deletion affected cell proliferation, we performed 24-hour pulse-chase labeling of BrdU at E12.5. We detected three stripes of BrdU+ cell aggregates parallel to the ventricular surface in the thalamus in wild-type embryos at E13.5 (Fig. 6A,A'). In *Gbx2*-KO embryos, although the three stripes of BrdU+ cells were still discernible in the ventral/anterior part of the thalamus, they collapsed into one, similar to that found in the epithalamus, in the dorsal/posterior part of the thalamus (Fig. 6B,B'). Furthermore, the innermost stripe of BrdU+ cells in the ventricular zone was markedly thinner in the *Gbx2*-KO thalamus at E13.5 (Fig. 6B'). By chase labeling for 7 hours with BrdU, we showed that numbers of BrdU+ cells were significantly reduced in both the VZ and SVZ of the thalamus, particularly prominent near the junction between the thalamus and epithalamus (Fig. 6C-G). The number of cells marked by phosphorylated histone 3 (pH3), which marks cells undergoing mitotic division, was not statistically different between the wild-type and *Gbx2*-KO thalamus (Fig. 6C-D,H). Collectively, our results show that loss of *Gbx2* alters the proliferation and neurogenic progression in the thalamus.

Cell non-autonomous function of Gbx2 in regulating neurogenic progression in the thalamus

Given that *Gbx2* is induced in postmitotic neural precursors, the abnormal cell proliferation in the *Gbx2*-KO thalamus suggests that Gbx2 regulates progression of thalamic progenitors by feedback signaling from postmitotic cells. Indeed, our gene expression analyses revealed that *Gbx2* deletion altered gene expression not only in the mantle zone, but also the intermediate and even the VZ of the thalamus (Fig. 5 and 7). For example, loss of *Gbx2* increased the expression of *Cntn2* and *Ebf3* in the intermediate domains between the mantle and ventricular zone of the thalamus in *Gbx2*-KO embryos at E12.5 (Fig. 7A,B,D,E). *H2afj*, which codes for an atypical histone protein (Nishida et al., 2005), is expressed throughout the VZ of the neural tube (Fig. 7G). *H2afj* transcripts were notably reduced in the thalamus particularly in the dorsal-most region of the *Gbx2*-KO thalamus at E13.5 (Fig. 7H). We have previously demonstrated a cell non-autonomous function of *Gbx2* in the establishment of the compartment boundary between the thalamus and epithalamus using chimeras and mosaics (Chen et al., 2009). Using the same approach as described previously (Chen et al., 2009; Chatterjee et al., 2012), we administrated tamoxifen to E10.5 $Gbx2^{creER/F}$ embryos so that creER-mediated recombination rendered the genotype of *Gbx2*-expressing cells from $Gbx2^{creER/F}$ to $Gbx2^{creER/-}$ in a mosaic manner. Remarkably, the normal expression of

Cntn2, *Ebf3* and *H2afj* was restored in E13.5 *Gbx2*$^{creER/F}$ embryos that received tamoxifen at E10.5 (Fig. 7C,F,I). We were unable to directly verify the loss of Gbx2 protein because of a lack of workable anti-Gbx2 antibodies. We thus explored a different approach by analyzing downstream targets of Gbx2. In agreement with the ISH data (Fig. 5B), immunostaining showed elevated expression of Cntn2 and Islr2 in the thalamus of *Gbx2*-KO embryos at E12.5 (Fig. 7J,K,M). Importantly, Cntn2 immunoreactivity was mostly absent in the thalamus of E12.5 *Gbx2*$^{creER/F}$ embryos that were given tamoxifen at E10.5 (Fig. 7L,N). By contrast, Islr2+ cells persisted and exhibited the salt-and-pepper mosaic pattern in the thalamus (Fig. 7L,N). Using a *Gbx2* RNA probe that recognizes sequence that is flanked by the two *loxP* sites of the *Gbx2*^{F} allele, we showed mosaic deletion of *Gbx2* transcripts in the mantle zone following tamoxifen administration, including the area where ectopic Cntn2 and Islr2 expression was detected in *Gbx2*-null embryos at E12.5 (Fig. 7 and S4). These findings demonstrate that Islr2 and Cntn2 are differentially regulated by the cell autonomous and non-autonomous function of Gbx2, respectively. Therefore, our data indirectly verify the presence of wild-type and *Gbx2*-deficient cells, which are respectively indicated by Islr2− and Islr2+ cells, in the thalamus of *Gbx2*$^{creER/F}$ embryos that were given tamoxifen at E10.5. Finally, BrdU pulse labeling revealed that cell proliferation was also rescued in *Gbx2* mosaic-deletion embryos at E13.5 (Fig. 7O-Q). Collectively, these data demonstrate that *Gbx2* plays a cell non-autonomous role in regulating proliferation and progression of progenitors in the developing thalamus.

DISCUSSION

In the current study, we have performed microarray analysis to compare the transcriptome of the thalamus between wild-type and *Gbx2*-deficient embryos at E12.5. To the best of our knowledge (based on information in the GEO database), this is the first attempt to capture the expression profile of the embryonic thalamus in mice. We show that *Gbx2* is essential for acquisition of the molecular identity of the thalamus. Interestingly, the loss of the thalamic identity due to *Gbx2* ablation is associated with a partial switch to the habenular identity. Moreover, *Gbx2* controls a feedback mechanism from postmitotic cells in the mantle zone to regulate the development of thalamic progenitor cells. Our new findings explain the profound defect in the developing thalamus due to the loss of *Gbx2*, and shed light on the molecular mechanism underlying the subdivision of the epithalamus and thalamus from a single developmental compartment in the diencephalon.

Despite the differences in cytoarchitecture and connectivity between thalamic and habenular neurons, the molecular mechanism underlying their specification and differentiation remains largely unknown. Our efforts through microarray analysis and expression database inspection have failed to identify molecular markers that distinguish the progenitor domains between the epithalamus and thalamus. By contrast, neural precursors arising from the prospective epithalamus and thalamus express markedly different transcriptional profiles at the onset of neurogenesis (Chatterjee et al., 2014)(Fig. 2,3,5). *Gbx2* is one of the earliest genes that are induced as neural cells exit the cell cycle in the thalamus (Bulfone et al., 1993; Nakagawa and O'Leary, 2003; Chen et al., 2009). Here, we show that inactivation of *Gbx2* prevents thalamic neurons from acquiring the thalamic identity and results in a partial conversion from thalamic to habenular molecular features. This cell-identity switch may

account for the profound defects found in the thalamus lacking *Gbx2*, particularly in the misrouting of thalamic axons to the ventral midbrain and hindbrain (Chatterjee et al., 2012), and in the abnormal contribution of thalamus-derived neurons to the habenula due to the loss of *Gbx2* (Chen et al., 2009). Therefore, *Gbx2* plays a crucial role in the subdivision of the epithalamus and thalamus within the P2 compartment by suppressing the habenular identity.

Irx genes are important for pattern formation and cell fate decision (Scholpp and Lumsden, 2010; Chatterjee and Li, 2012). Prior studies have demonstrated the important roles of *Irx1* and *Irx3* in development of the diencephalon (Scholpp et al., 2007; Rodriguez-Seguel et al., 2009; Robertshaw et al., 2013). By comparing *Irx1* expression at different positions of the developing thalamus along the anterior and posterior axis, we show that *Irx1* is initially expressed throughout the P2 domain and down-regulated in neuronal precursors as they exit the cell cycle and turn on *Gbx2* transcription. Importantly, by studying mouse embryos lacking *Gbx2* or both *Gbx2* and *Pax6*, we demonstrate that *Gbx2* inhibits *Irx* genes in the thalamus (Fig. 2). In both mice and humans, the six *Irx* genes are grouped into two genomic clusters, IrxA (*Irx1/2/4*) and IrxB (*Irx3/5/6*) (Peters et al., 2000). Interestingly, *Irx1/2/3/5* are similarly expressed in the epithalamus and the ventricular zone of the thalamus; in the absence of *Gbx2*, these four genes were ectopically expressed in postmitotic cells of the thalamus (Fig. 2 and data not shown), suggesting that *Irx1/2/3/5*, but not *Irx4/6*, may be controlled by common regulatory elements present in both clusters. One of the recurring themes of *Irx* function is to define distinct competence for inductive signals in regionalization of the neural epithelium (Kobayashi et al., 2002; Robertshaw et al., 2013). Therefore, the repression of *Irx* genes from the postmitotic thalamic cells may be essential for a switch from the habenular to thalamic developmental program, probably by changing the competence of thalamic precursor cells to inductive signals. This notion will be tested in future studies.

In agreement with a delay in the onset of neurogenesis in the thalamus compared to the epithalamus, robust expression of *Nefm* and *Dcx*, indicative of postmitotic neurons, is present in the epithalamus but not the thalamus at E12.5 (Fig. 3,5). Furthermore, *Id4* and *Ebf3*, which have opposing roles in neurogenesis, are differentially expressed in the epithalamus and thalamus (Fig. 3,5). Deletion of *Gbx2* leads to precocious expression of *Nefm*, *Dcx*, and *Ebf3* and blocks Id4 expression in the thalamus. The loss of *Gbx2* also affects cell proliferation in the thalamic VZ, particularly in the area near the epithalamus and thalamus border (Fig. 6). Therefore, the thalamus adopts not only a molecular signature but also neurogenic pattern that resemble those of the epithalamus in the absence of *Gbx2*. In zebrafish embryos, the neurogenetic gradient in the thalamus is controlled by *her6*, through interacting with *neurog1* and *coe2* (an *Ebf* gene) (Scholpp et al., 2009). We found no significant changes in the mRNA level of *Hes* genes, including *Hes1*–the *her6* orthologue, in the thalamus due to *Gbx2* deletion. ICH showed that Hes1 expression in the thalamus was indistinguishable between wild-type and *Gbx2*-KO embryos at E12.5 (Fig. S3). Therefore, *Gbx2* regulates neurogenesis in the thalamus through a *Hes1*-independent pathway. Using genetic mosaics, we demonstrate that *Gbx2* has a cell non-autonomous function probably by controlling a feedback mechanism to regulate cell proliferation and neurogenic progression in the thalamus. The precise mechanism underlying the cell non-autonomous function of

Gbx2 remains to be determined. Examination of the list of DE genes has not revealed an obvious candidate. Interestingly, we have recently shown that Shh signaling has a long-range effect in the partitioning of P2 into the epithalamus and thalamus, and reduction of Shh signaling results in expansion of the epithalamus at the expense of the thalamus (Chatterjee et al., 2014). Therefore, *Gbx2* may participate in the regulation of the range of Shh function during differentiation between the thalamus and epithalamus. To explore this hypothesis further, more extensive transcriptome study using RNA-Seq technology may be required to discover *Gbx2* downstream targets that are involved in modulation of Shh signaling.

Supplementary Material

Refer to Web version on PubMed Central for supplementary material.

ACKNOWLEDGEMENTS

We thank Drs. Alan W. Leung and Iftekher Naser for their critical reading and comments on the manuscript. We thank Dr. Yashushi Nakagawa, David Ginty for providing the antibodies against Dbx1 and Islr2, Drs. Eric Turner and Chi-Chung Hui for providing *Ebf3* expressing vector and cDNAs for *Irx1,Irx2 and Irx3*, respectively. The monoclonal anti-neurofilament antibody (2H3) was developed by T.M. Jessell and J. Dodd, and obtained through the Developmental Studies Hybridoma Bank under the auspices of the NICHD and maintained by The University of Iowa (Iowa City, IA). This work was supported by a grant from the National Institute of Health (R01MH094914).

REFERENCES

Angevine JB Jr. Time of neuron origin in the diencephalon of the mouse. An autoradiographic study. J Comp Neurol. 1970; 139:129–187. [PubMed: 5463599]

Bai G, Sheng N, Xie Z, Bian W, Yokota Y, Benezra R, Kageyama R, Guillemot F, Jing N. Id sustains Hes1 expression to inhibit precocious neurogenesis by releasing negative autoregulation of Hes1. Dev Cell. 2007; 13:283–297. [PubMed: 17681138]

Bedford L, Walker R, Kondo T, van Cruchten I, King ER, Sablitzky F. Id4 is required for the correct timing of neural differentiation. Dev Biol. 2005; 280:386–395. [PubMed: 15882580]

Belliveau MJ, Cepko CL. Extrinsic and intrinsic factors control the genesis of amacrine and cone cells in the rat retina. Development. 1999; 126:555–566. [PubMed: 9876184]

Bluske KK, Vue TY, Kawakami Y, Taketo MM, Yoshikawa K, Johnson JE, Nakagawa Y. beta-Catenin signaling specifies progenitor cell identity in parallel with Shh signaling in the developing mammalian thalamus. Development. 2012; 139:2692–2702. [PubMed: 22745311]

Bulfone A, Puelles L, Porteus MH, Frohman MA, Martin GR, Rubenstein JL. Spatially restricted expression of Dlx-1, Dlx-2 (Tes-1), Gbx-2, and Wnt-3 in the embryonic day 12.5 mouse forebrain defines potential transverse and longitudinal segmental boundaries. J Neurosci. 1993; 13:3155–3172. [PubMed: 7687285]

Chatterjee M, Li JY. Patterning and compartment formation in the diencephalon. Front Neurosci. 2012; 6:66. [PubMed: 22593732]

Chatterjee M, Guo Q, Weber S, Scholpp S, Li JY. Pax6 regulates the formation of the habenular nuclei by controlling the temporospatial expression of Shh in the diencephalon in vertebrates. BMC Biol. 2014; 12:13. [PubMed: 24528677]

Chatterjee M, Li K, Chen L, Maisano X, Guo Q, Gan L, Li JY. Gbx2 regulates thalamocortical axon guidance by modifying the LIM and Robo codes. Development. 2012; 139:4633–4643. [PubMed: 23136391]

Chen L, Guo Q, Li JY. Transcription factor Gbx2 acts cell-nonautonomously to regulate the formation of lineage-restriction boundaries of the thalamus. Development. 2009; 136:1317–1326. [PubMed: 19279136]

Cohen DR, Cheng CW, Cheng SH, Hui CC. Expression of two novel mouse Iroquois homeobox genes during neurogenesis. Mech Dev. 2000; 91:317–321. [PubMed: 10704856]

Du P, Kibbe WA, Lin SM. lumi: a pipeline for processing Illumina microarray. Bioinformatics. 2008; 24:1547–1548. [PubMed: 18467348]

Finger JH, Smith CM, Hayamizu TF, McCright IJ, Eppig JT, Kadin JA, Richardson JE, Ringwald M. The mouse Gene Expression Database (GXD): 2011 update. Nucleic Acids Res. 2011; 39:D835–841. [PubMed: 21062809]

Flames N, Hobert O. Gene regulatory logic of dopamine neuron differentiation. Nature. 2009; 458:885–889. [PubMed: 19287374]

Garel S, Marin F, Grosschedl R, Charnay P. Ebf1 controls early cell differentiation in the embryonic striatum. Development. 1999; 126:5285–5294. [PubMed: 10556054]

Hamburger V, Hamilton HL. A series of normal stages in the development of the chick embryo. J Morphol. 1951; 88:49–92. [PubMed: 24539719]

Hevner RF, Miyashita-Lin E, Rubenstein JL. Cortical and thalamic axon pathfinding defects in Tbr1, Gbx2, and Pax6 mutant mice: evidence that cortical and thalamic axons interact and guide each other. J Comp Neurol. 2002; 447:8–17. [PubMed: 11967891]

Hikosaka O. The habenula: from stress evasion to value-based decision-making. Nature reviews Neuroscience. 2010; 11:503–513. [PubMed: 20559337]

Hikosaka O, Sesack SR, Lecourtier L, Shepard PD. Habenula: crossroad between the basal ganglia and the limbic system. J Neurosci. 2008; 28:11825–11829. [PubMed: 19005047]

Hirata T, Nakazawa M, Muraoka O, Nakayama R, Suda Y, Hibi M. Zinc-finger genes Fez and Fez-like function in the establishment of diencephalon subdivisions. Development. 2006; 133:3993–4004. [PubMed: 16971467]

Hobert O. Regulatory logic of neuronal diversity: terminal selector genes and selector motifs. Proc Natl Acad Sci U S A. 2008; 105:20067–20071. [PubMed: 19104055]

Hobert O. Maintaining a memory by transcriptional autoregulation. Curr Biol. 2011; 21:R146–147. [PubMed: 21334290]

Huang da W, Sherman BT, Lempicki RA. Systematic and integrative analysis of large gene lists using DAVID bioinformatics resources. Nat Protoc. 2009; 4:44–57. [PubMed: 19131956]

Jeong Y, Dolson DK, Waclaw RR, Matise MP, Sussel L, Campbell K, Kaestner KH, Epstein DJ. Spatial and temporal requirements for sonic hedgehog in the regulation of thalamic interneuron identity. Development. 2011; 138:531–541. [PubMed: 21205797]

Johnson WE, Li C, Rabinovic A. Adjusting batch effects in microarray expression data using empirical Bayes methods. Biostatistics. 2007; 8:118–127. [PubMed: 16632515]

Jones, EG. The thalamus. 2nd Edition.. Cambridge University Press; Cambridge ; New York: 2007.

Jones EG, Rubenstein JL. Expression of regulatory genes during differentiation of thalamic nuclei in mouse and monkey. J Comp Neurol. 2004; 477:55–80. [PubMed: 15281080]

Kataoka A, Shimogori T. Fgf8 controls regional identity in the developing thalamus. Development. 2008; 135:2873–2881. [PubMed: 18653561]

Kiecker C, Lumsden A. Hedgehog signaling from the ZLI regulates diencephalic regional identity. Nat Neurosci. 2004; 7:1242–1249. [PubMed: 15494730]

Kobayashi D, Kobayashi M, Matsumoto K, Ogura T, Nakafuku M, Shimamura K. Early subdivisions in the neural plate define distinct competence for inductive signals. Development. 2002; 129:83–93. [PubMed: 11782403]

Lecourtier L, Kelly PH. A conductor hidden in the orchestra? Role of the habenular complex in monoamine transmission and cognition. Neuroscience and biobehavioral reviews. 2007; 31:658–672. [PubMed: 17379307]

Li K, Zhang J, Li JY. Gbx2 plays an essential but transient role in the formation of thalamic nuclei. PLoS One. 2012; 7:e47111. [PubMed: 23056596]

Mandai K, Guo T, St Hillaire C, Meabon JS, Kanning KC, Bothwell M, Ginty DD. LIG family receptor tyrosine kinase-associated proteins modulate growth factor signals during neural development. Neuron. 2009; 63:614–627. [PubMed: 19755105]

Martinez-Ferre A, Martinez S. The development of the thalamic motor learning area is regulated by Fgf8 expression. J Neurosci. 2009; 29:13389–13400. [PubMed: 19846726]

McAllister JP II, Das GD. Neurogenesis in the epithalamus, dorsal thalamus and ventral thalamus of the rat: an autoradiographic and cytological study. J Comp Neurol. 1977; 172:647–686. [PubMed: 838894]

Miyashita-Lin EM, Hevner R, Wassarman KM, Martinez S, Rubenstein JL. Early neocortical regionalization in the absence of thalamic innervation. Science. 1999; 285:906–909. [PubMed: 10436162]

Nakagawa Y, O'Leary DD. Combinatorial expression patterns of LIM-homeodomain and other regulatory genes parcellate developing thalamus. J Neurosci. 2001; 21:2711–2725. [PubMed: 11306624]

Nakagawa Y, O'Leary DD. Dynamic patterned expression of orphan nuclear receptor genes RORalpha and RORbeta in developing mouse forebrain. Dev Neurosci. 2003; 25:234–244. [PubMed: 12966220]

Nishida H, Suzuki T, Tomaru Y, Hayashizaki Y. A novel replication-independent histone H2a gene in mouse. BMC Genet. 2005; 6:10. [PubMed: 15720718]

Olsen SK, Li JY, Bromleigh C, Eliseenkova AV, Ibrahimi OA, Lao Z, Zhang F, Linhardt RJ, Joyner AL, Mohammadi M. Structural basis by which alternative splicing modulates the organizer activity of FGF8 in the brain. Genes Dev. 2006; 20:185–198. [PubMed: 16384934]

Peters T, Dildrop R, Ausmeier K, Ruther U. Organization of mouse Iroquois homeobox genes in two clusters suggests a conserved regulation and function in vertebrate development. Genome Res. 2000; 10:1453–1462. [PubMed: 11042145]

Puelles E, Acampora D, Gogoi R, Tuorto F, Papalia A, Guillemot F, Ang SL, Simeone A. Otx2 controls identity and fate of glutamatergic progenitors of the thalamus by repressing GABAergic differentiation. J Neurosci. 2006; 26:5955–5964. [PubMed: 16738237]

Puelles L, Rubenstein JL. Forebrain gene expression domains and the evolving prosomeric model. Trends Neurosci. 2003; 26:469–476. [PubMed: 12948657]

Quina LA, Wang S, Ng L, Turner EE. Brn3a and Nurr1 mediate a gene regulatory pathway for habenula development. J Neurosci. 2009; 29:14309–14322. [PubMed: 19906978]

Ritchie ME, Phipson B, Wu D, Hu Y, Law CW, Shi W, Smyth GK. limma powers differential expression analyses for RNA-sequencing and microarray studies. Nucleic Acids Res. 2015; 43:e47. [PubMed: 25605792]

Robertshaw E, Matsumoto K, Lumsden A, Kiecker C. Irx3 and Pax6 establish differential competence for Shh-mediated induction of GABAergic and glutamatergic neurons of the thalamus. Proc Natl Acad Sci U S A. 2013; 110:E3919–3926. [PubMed: 24065827]

Rodriguez-Seguel E, Alarcon P, Gomez-Skarmeta JL. The Xenopus Irx genes are essential for neural patterning and define the border between prethalamus and thalamus through mutual antagonism with the anterior repressors Fezf and Arx. Dev Biol. 2009; 329:258–268. [PubMed: 19268445]

Rubenstein JL, Martinez S, Shimamura K, Puelles L. The embryonic vertebrate forebrain: the prosomeric model. Science. 1994; 266:578–580. [PubMed: 7939711]

Scholpp S, Lumsden A. Building a bridal chamber: development of the thalamus. Trends Neurosci. 2010; 33:373–380. [PubMed: 20541814]

Scholpp S, Wolf O, Brand M, Lumsden A. Hedgehog signalling from the zona limitans intrathalamica orchestrates patterning of the zebrafish diencephalon. Development. 2006; 133:855–864. [PubMed: 16452095]

Scholpp S, Foucher I, Staudt N, Peukert D, Lumsden A, Houart C. Otx1l, Otx2 and Irx1b establish and position the ZLI in the diencephalon. Development. 2007; 134:3167–3176. [PubMed: 17670791]

Scholpp S, Delogu A, Gilthorpe J, Peukert D, Schindler S, Lumsden A. Her6 regulates the neurogenetic gradient and neuronal identity in the thalamus. Proc Natl Acad Sci U S A. 2009; 106:19895–19900. [PubMed: 19903880]

Seuntjens E, Nityanandam A, Miquelajauregui A, Debruyn J, Stryjewska A, Goebbels S, Nave KA, Huylebroeck D, Tarabykin V. Sip1 regulates sequential fate decisions by feedback signaling from postmitotic neurons to progenitors. Nat Neurosci. 2009; 12:1373–1380. [PubMed: 19838179]

Sherman, SM.; Guillery, RW. Exploring the thalamus and its role in cortical function. 2nd Edition.. MIT Press; Cambridge, Mass.: 2006.

Smart IH. Proliferative characteristics of the ependymal layer during the early development of the mouse diencephalon, as revealed by recording the number, location, and plane of cleavage of mitotic figures. J Anat. 1972; 113:109–129. [PubMed: 4648478]

Subramanian A, Tamayo P, Mootha VK, Mukherjee S, Ebert BL, Gillette MA, Paulovich A, Pomeroy SL, Golub TR, Lander ES, Mesirov JP. Gene set enrichment analysis: a knowledge-based approach for interpreting genome-wide expression profiles. Proc Natl Acad Sci U S A. 2005; 102:15545–15550. [PubMed: 16199517]

Thompson CL, et al. A high-resolution spatiotemporal atlas of gene expression of the developing mouse brain. Neuron. 2014; 83:309–323. [PubMed: 24952961]

Visel A, Thaller C, Eichele G. GenePaint.org: an atlas of gene expression patterns in the mouse embryo. Nucleic Acids Res. 2004; 32:D552–556. [PubMed: 14681479]

Vue TY, Bluske K, Alishahi A, Yang LL, Koyano-Nakagawa N, Novitch B, Nakagawa Y. Sonic hedgehog signaling controls thalamic progenitor identity and nuclei specification in mice. J Neurosci. 2009; 29:4484–4497. [PubMed: 19357274]

Vue TY, Aaker J, Taniguchi A, Kazemzadeh C, Skidmore JM, Martin DM, Martin JF, Treier M, Nakagawa Y. Characterization of progenitor domains in the developing mouse thalamus. J Comp Neurol. 2007; 505:73–91. [PubMed: 17729296]

Wang L, Bluske KK, Dickel LK, Nakagawa Y. Basal progenitor cells in the embryonic mouse thalamus - their molecular characterization and the role of neurogenins and Pax6. Neural Dev. 2011; 6:35. [PubMed: 22077982]

Wassarman KM, Lewandoski M, Campbell K, Joyner AL, Rubenstein JL, Martinez S, Martin GR. Specification of the anterior hindbrain and establishment of a normal mid/hindbrain organizer is dependent on Gbx2 gene function. Development. 1997; 124:2923–2934. [PubMed: 9247335]

Yun K, Mantani A, Garel S, Rubenstein J, Israel MA. Id4 regulates neural progenitor proliferation and differentiation in vivo. Development. 2004; 131:5441–5448. [PubMed: 15469968]

Zhou CJ, Pinson KI, Pleasure SJ. Severe defects in dorsal thalamic development in low-density lipoprotein receptor-related protein-6 mutants. J Neurosci. 2004; 24:7632–7639. [PubMed: 15342729]

HIGHLIGHTS

- Genome-wide transcriptome studies identify putative Gbx2 downstream targets.
- *Gbx2* inhibits expression of multiple *Iroquois* genes in the diencephalon.
- *Gbx2* promotes thalamic identity and represses habenular identity.
- *Gbx2* controls a feedback signaling from postmitotic cells to dividing progenitors.

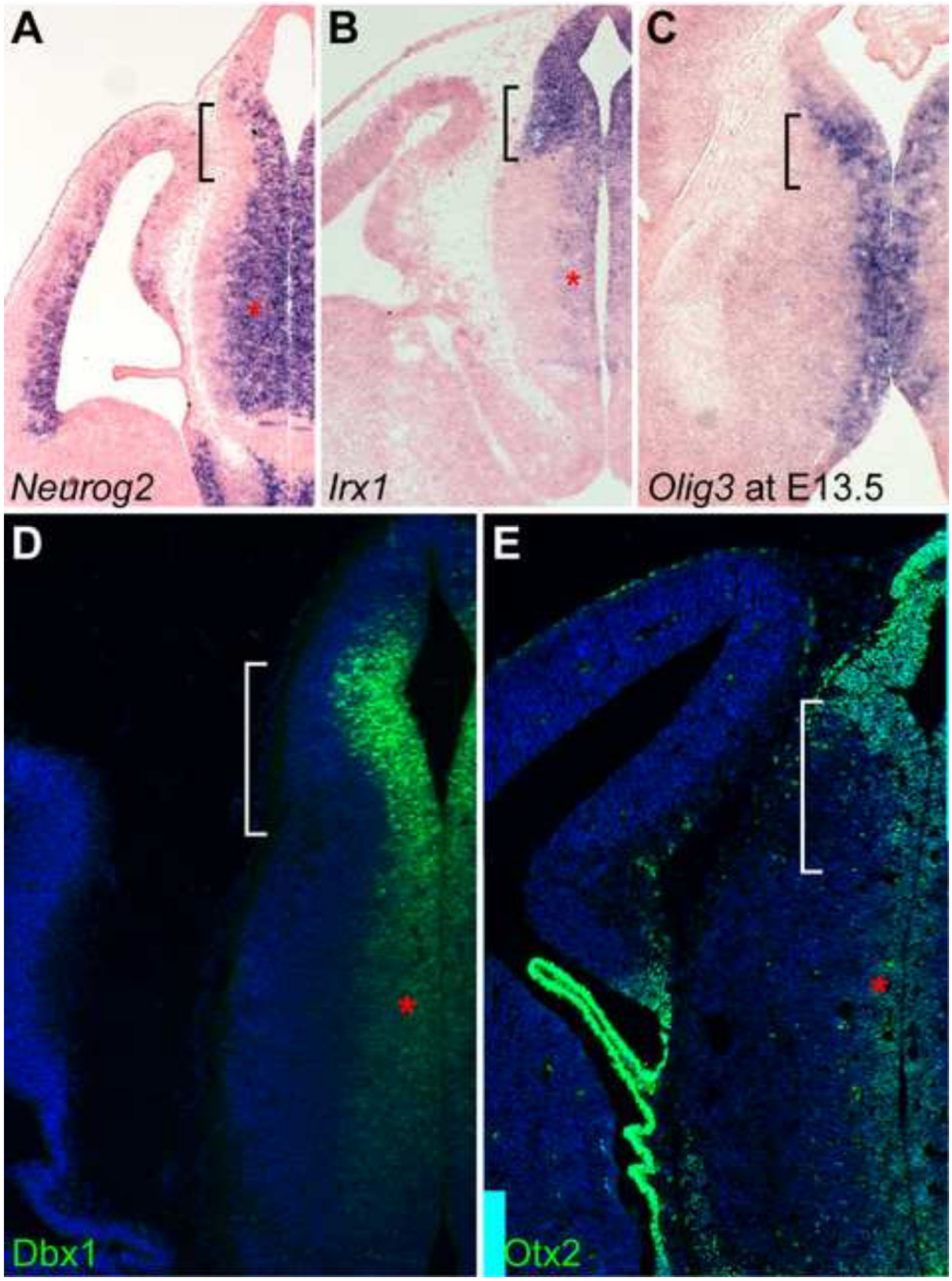

Figure 1. Progenitor cells in the P2 domain express common developmental regulator genes

(A-E) *In situ* hybridization (A-C) and immunostaining (D,E) on coronal sections of mouse brains at E12.5, except for C at E13.5. Probes and antibodies are indicated in the lower left corner of the image. The brackets and asterisks denote the epithalamus and the expression in the ventricular zone of the thalamus, respectively.

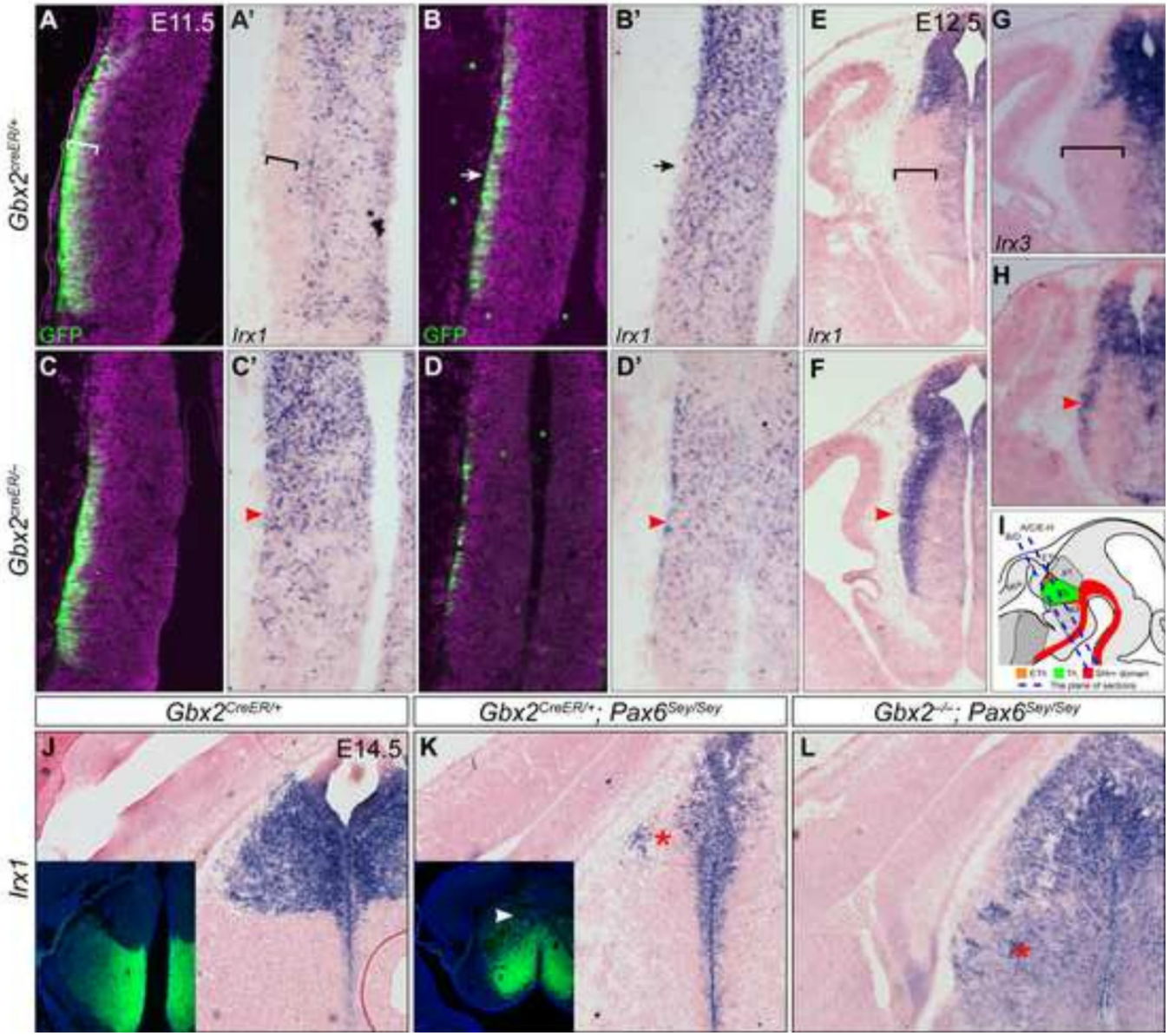

Figure 2. *Gbx2* represses *Irx* genes in postmitotic thalamic neurons

(A-F) Immunofluorescence and *in situ* hybridization on coronal sections of control and *Gbx2*-KO embryos at E11.5 (A-D') and E12.5 (E-H). Antibodies and probes are indicated at the lower left corner; genotypes to the left. (I) Illustration of mouse embryonic brain and the sectioning planes corresponding to A-H. Brackets indicate the GFP/Gbx2 positive and Irx negative domain; arrows show fewer GFP+ cells and remnants of *Irx1* transcripts in the anterior part of the thalamus; arrowheads denote the persistent *Irx* transcripts. (J-L) *In situ* hybridization for *Irx1* on coronal sections of E14.5 brain. Insets show immunostaining for GFP on adjacent sections to J and K respectively. The arrowhead indicates GFP expression in the presumptive habenula; asterisks show the loss (K) or gain (L) of *Irx1* expression, respectively.

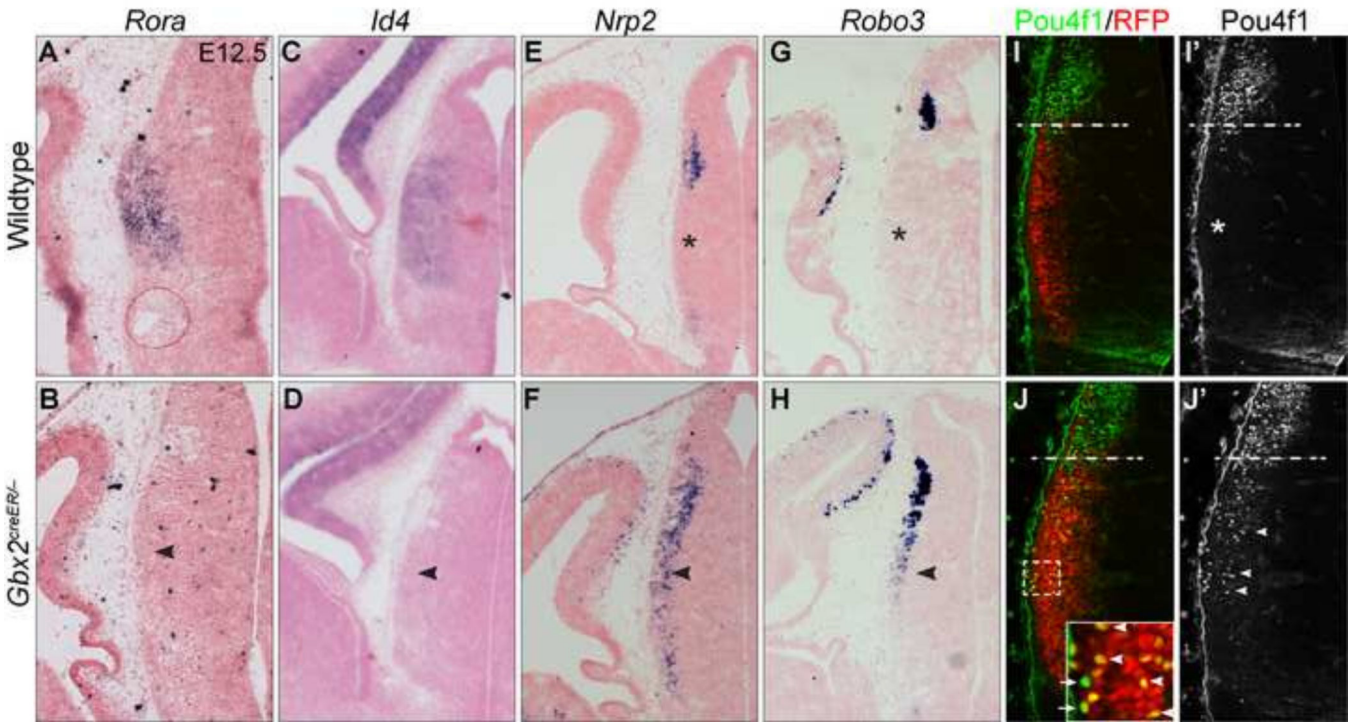

Figure 3. Deletion of *Gbx2* results in loss of thalamic-specific genes and ectopic expression of habenular markers in the thalamus

(A-J) *In situ* hybridization (A-H) and immunofluorescence (I-J') on coronal sections of the thalamus at E12.5. Probes and antibodies are indicated to the top; genotypes to the left. Asterisks show that absence of *Nrp2*, *Robo3* and Pou4f1 in the wild-type thalamus; arrowheads denote the abnormal expression in the *Gbx2*-KO thalamus; dashed lines demarcate the border between the thalamus and epithalamus. Note that the majority of Pou4f1+ cells are marked by RFP (arrowheads), and only a few Pou4f1+ cells (arrows) are negative for RFP in the *Gbx2*-KO thalamus. The boxed area is enlarged in the inset in J.

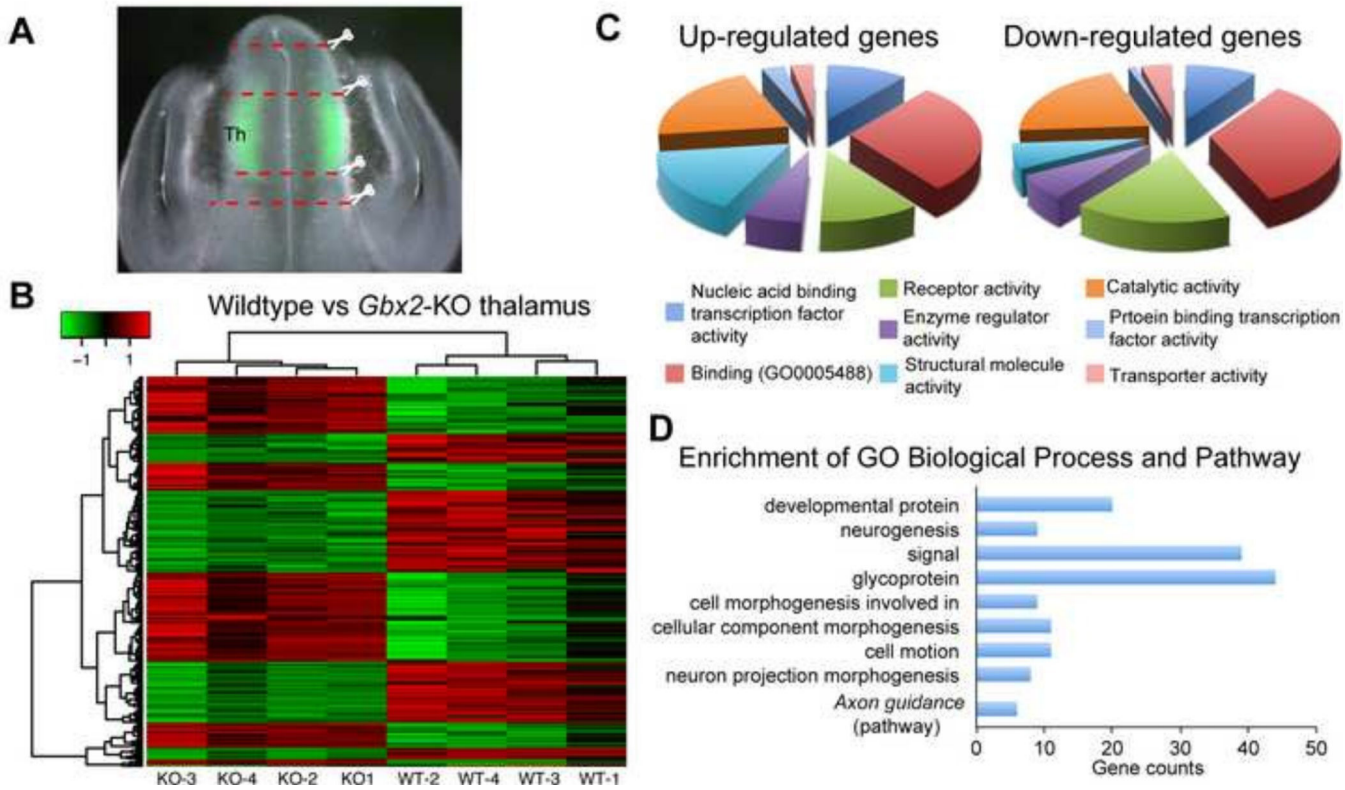

Figure 4. Genome-wide transcriptional profiling of wild-type and *Gbx2*-KO thalamus at E12.5

(A) Micro-dissection of the thalamus with the guide of GFP in E12.5 embryos carrying the *Gbx2*^{creER} allele. (B) Heatmap representation of the relative expression level and clustering of differentially expressed genes. (C,D) Diagram representation of enrichment for cellular processes (C) and biological and pathway (D) of *Gbx2* downstream genes.

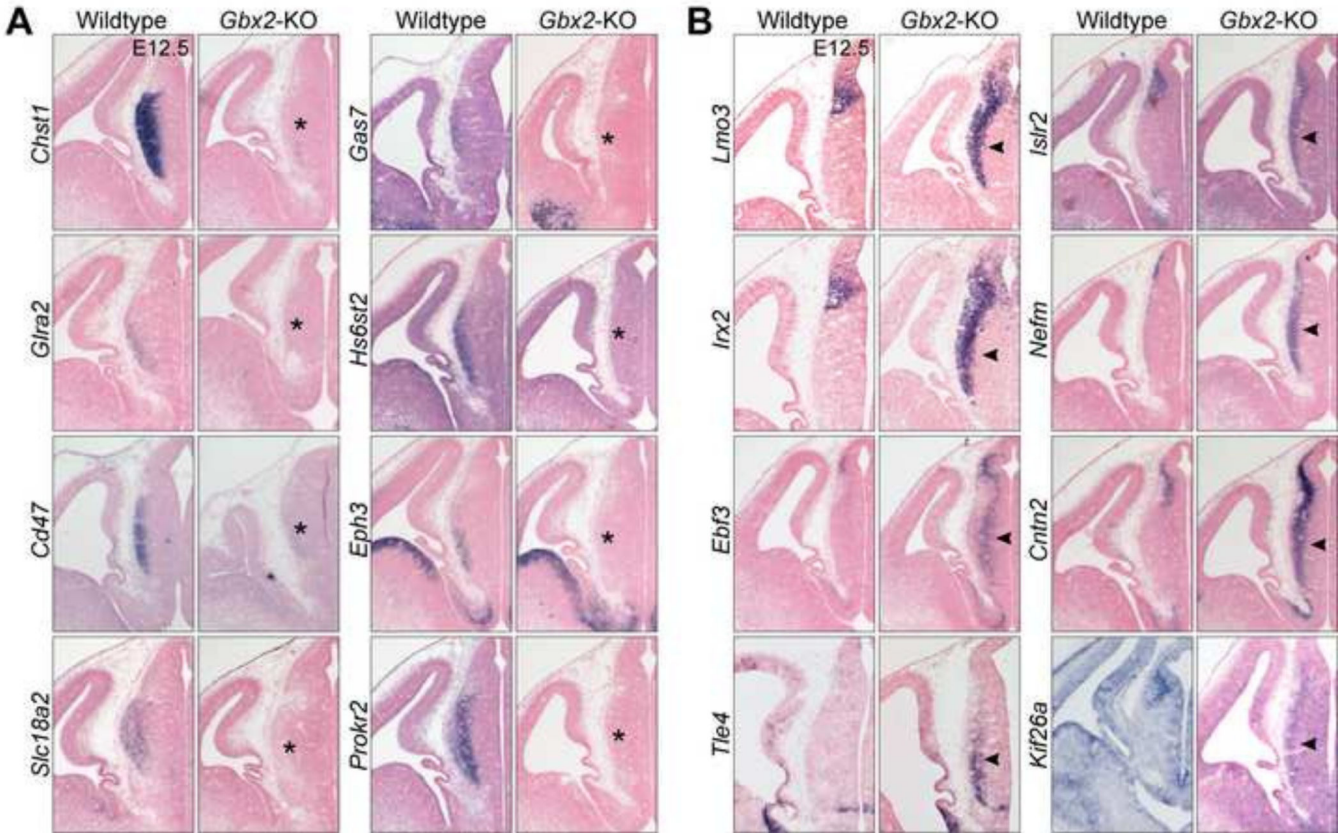

Figure 5. Verification of DE genes identified by microarrays

(A,B) *In situ* hybridization on coronal sections of the thalamus at E12.5. Probes and genotypes are indicated to the left and top, respectively. Note the loss of thalamic markers (asterisks in A) and gain of epithalamic ones (arrowheads in B) due to the loss of *Gbx2*.

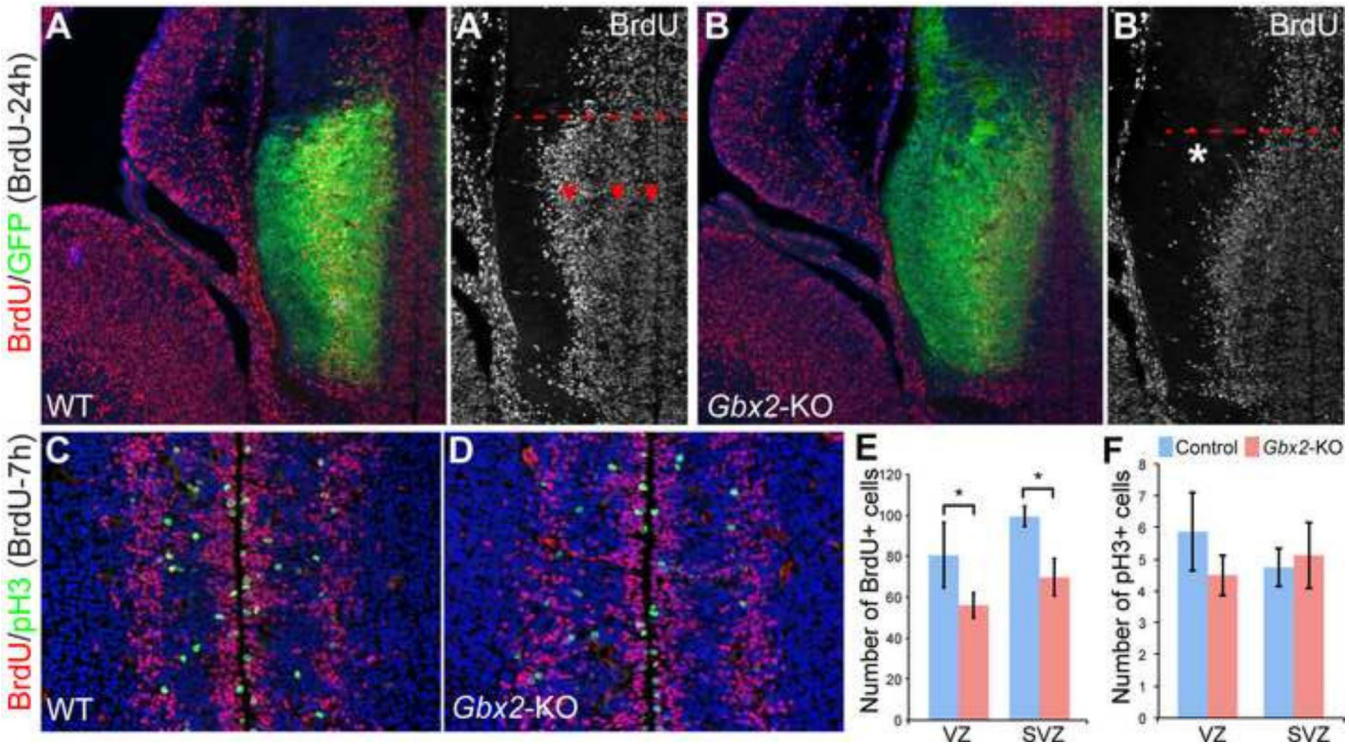

Figure 6. Loss of *Gbx2* causes abnormal cell proliferation in the thalamus

(A-F) Immunofluorescence on coronal sections of control and *Gbx2*-KO thalamus at E13.5 following BrdU chase or pulse labeling as indicated. Dashed lines demarcate the boundary between the thalamus and the epithalamus; arrowheads indicate the three stripes of BrdU+ cells parallel to the ventricular surface; the asterisk shows the abnormal curvature of the outer band of BrdU+ cells in the dorsal-most region of the thalamus due to the loss of *Gbx2*. (G-I) Histogram representation of quantification of proliferating and newly generated postmitotic cells. Asterisks indicate statistical significance ($p<0.05$, Student's t-test).

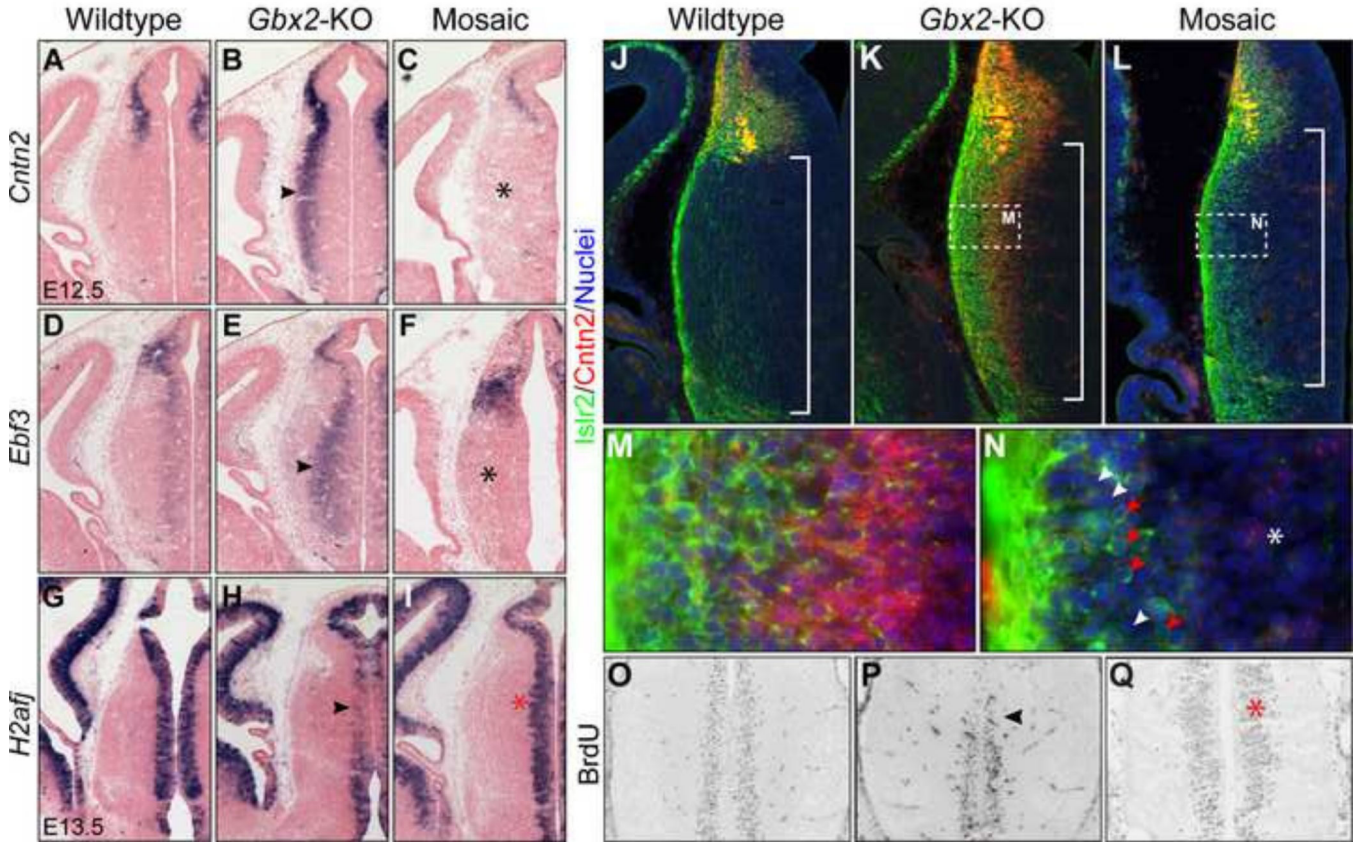

Figure 7. *Gbx2* act cell non-autonomously to regulate gene expression and cell proliferation

(A-I) *In situ* hybridization on coronal sections of the thalamus of indicated genotypes between E12.5 and E13.5. (J-N) Immunostaining of Islr2 and Cntn2 on coronal sections of the E12.5 thalamus. Brackets demarcate the thalamus; red arrowheads indicate Islr2^{+}, presumably *Gbx2*-deficient cells; white arrowheads indicate Islr2^{-}, presumably wild-type cells. (O-W) Immunostaining of BrdU on coronal sections of E13.5 thalamus following 1-hour pulse labeling. The arrowhead indicates the abnormal gene expression and cell proliferation in *Gbx2*-KO thalamus; the asterisk shows the rescue in the thalamus that is composed of wild-type and *Gbx2*-deficient cells.

Table I

Down-regulated genes due to the loss of *Gbx2*

key	Symbol	Description	logFC	adj.P.Val	Expression	Verified
Combined	Cyp1b1	cytochrome P450, family 1, subfamily b, polypeptide 1	−3.0	0.004	NA	
Array2	Cops8	COP9 (constitutive photomorphogenic) homolog, subunit 8 (Arabidopsis thaliana)	−2.7	0.020	NA	
Combined	Id4	inhibitor of DNA binding 4	−2.5	0.003	Yes	Yes
Array1	Chst1	carbohydrate (keratan sulfate Gal-6) sulfotransferase 1	−2.4	0.001	Yes	Yes
Combined	Ntng1	netrin G1	−2.1	0.005	Yes	Yes*
Array1	Rbfox1	RNA binding protein, fox-1 homolog (C. elegans) 1	−2.1	0.015	Yes	
Combined	Kirrel3	kin of IRRE like 3 (Drosophila)	−2.0	0.011	Yes	
Combined	Glra2	glycine receptor, alpha 2 subunit	−2.0	0.014	Yes	Yes
Combined	Hs6st2	heparan sulfate 6-O-sulfotransferase 2	−1.9	0.004	Yes	Yes
Array1	Sertad4	SERTA domain containing 4	−1.9	0.002	NA	IC
Array1	C1ql2	complement component 1, q subcomponent-like 2	−1.9	0.027	PTh	
Combined	Slc18a2	solute carrier family 18 (vesicular monoamine), member 2	−1.8	0.008	Yes	Yes
Array2	Gbx2	gastrulation brain homeobox 2	−1.8	0.044	Yes	Yes**
Array1	Hbb-b1	hemoglobin, beta adult major chain	−1.8	0.086	NA	
Combined	Calb2	calbindin 2	−1.8	0.005	Yes	
Combined	Rora	RAR-related orphan receptor alpha	−1.8	0.013	Yes	Yes
Array2	Sema3a	sema domain, immunoglobulin domain (Ig), short basic domain, secreted, (semaphorin) 3A	−1.7	0.074	Yes	
Combined	Nxph1	neurexophilin 1	−1.7	0.047	Yes	
Array1	Wif1	Wnt inhibitory factor 1	−1.6	0.028	Yes	Yes*
Array1	Ttc27	tetratricopeptide repeat domain 27	−1.6	0.026	NA	
Array1	Sulf2	sulfatase 2	−1.6	0.003	?	
Combined	Rit2	Ras-like without CAAX 2	−1.6	0.011	Yes	
Array1	Dlk1	delta-like 1 homolog (Drosophila)	−1.6	0.046	Yes	IC
Combined	Samd5	sterile alpha motif domain containing 5	−1.5	0.005	Yes	
Array1	Robo2	roundabout homolog 2 (Drosophila)	−1.5	0.034	Th	Yes**
Array2	Tle1	transducin-like enhancer of split 1, homolog of Drosophila E(spl)	−1.4	0.038	PTh	
Array1	Dab1	disabled 1	−1.3	0.007	Yes	Yes*
Combined	Thsd7b	thrombospondin, type I, domain containing 7B	−1.3	0.015	NA	
Combined	Sgk1	serum/glucocorticoid regulated kinase 1	−1.3	0.009	Yes	
Combined	Syt13	synaptotagmin XIII	−1.3	0.005	Yes	
Array1	Clmp	CXADR-like membrane protein	−1.3	0.025	NA	
Array1	Foxp2	forkhead box P2	−1.3	0.026	Yes	Yes*
Combined	Gm10304	predicted gene 10304	−1.2	0.021		
Combined	Cd47	CD47 antigen (Rh-related antigen, integrin-associated signal transducer)	−1.2	0.030	Yes	Yes
Combined	Ccng2	cyclin G2	−1.2	0.027	NA	

key	Symbol	Description	logFC	adj.P.Val	Expression	Verified
Combined	Tenm4	teneurin transmembrane protein 4	−1.2	0.025	Yes	
Array2	Vegfc	vascular endothelial growth factor C	−1.2	0.053	Yes	
Array1	Lhfp	lipoma HMGIC fusion partner	−1.1	0.039	Yes	
Combined	Chn2	chimerin 2	−1.1	0.024		
Array2	Cfap69	cilia and flagella associated protein 69	−1.1	0.065	No signals	
Combined	Fgfr1op2	FGFR1 oncogene partner 2	−1.1	0.023		
Combined	Pcdh9	protocadherin 9	−1.1	0.041	Yes	
Array1	Ednrb	endothelin receptor type B	−1.1	0.026	No signals	
Array1	Vcam1	vascular cell adhesion molecule 1	−1.1	0.061	No signals	
Array2	Enpp2	ectonucleotide pyrophosphatase/phosphodiesterase 2	−1.1	0.078		
Combined	Slc1a3	solute carrier family 1 (glial high affinity glutamate transporter), member 3	−1.0	0.024	Yes	
Combined	Atrnl1	attractin like 1	−1.0	0.027	NA	
Array1	Rnf152	ring finger protein 152	−1.0	0.041	Yes	
Combined	Arpp21	cyclic AMP-regulated phosphoprotein, 21	−1.0	0.034	Yes	
Combined	Sel1l3	sel-1 suppressor of lin-12-like 3 (C. elegans)	−1.0	0.011		
Combined	Rgs10	regulator of G-protein signalling 10	−1.0	0.044	NA	
Array1	Brat1	BRCA1-associated ATM activator 1	−0.9	0.028	NA	
Array1	Zfhx4	zinc finger homeodomain 4	−0.9	0.089	No signals	
Array1	Lxn	latexin	−0.9	0.032	Yes (VZ)	
Array1	Dner	delta/notch-like EGF-related receptor	−0.9	0.078	Not specific	
Array1	Celf2	CUGBP, Elav-like family member 2	−0.9	0.080	Yes	
Array1	Fam155a	family with sequence similarity 155, member A	−0.9	0.028	No signals	
Array1	Pmp22	peripheral myelin protein 22	−0.9	0.041	NA	
Combined	Igsf21	immunoglobulin superfamily, member 21	−0.9	0.018	Yes	
Array1	Elmo1	engulfment and cell motility 1	−0.9	0.026	Yes	
Combined	Glce	glucuronyl C5-epimerase	−0.9	0.033	Yes	
Array1	Dkk3	dickkopf homolog 3 (Xenopus laevis)	−0.9	0.027	Not specific	
Array1	Tmem130	transmembrane protein 130	−0.9	0.096	Not specific	
Array1	Rapgef5	Rap guanine nucleotide exchange factor (GEF) 5	−0.9	0.028	Yes	
Array1	Tmem108	transmembrane protein 108	−0.9	0.030	No signals	
Array1	Limch1	LIM and calponin homology domains 1	−0.9	0.063	No signals	
Combined	Epha3	Eph receptor A3	−0.9	0.046	Yes	Yes
Combined	Gpr83	G protein-coupled receptor 83	−0.8	0.048	weak signals	
Array1	Arrdc3	arrestin domain containing 3	−0.8	0.036	NA	
Combined	Prmt8	protein arginine N-methyltransferase 8	−0.8	0.025	NA	
Array1	E130114P18Ri	RIKEN cDNA E130114P18 gene	−0.8	0.079	NA	
Array1	Bcl11a	B cell CLL/lymphoma 11A (zinc finger protein)	−0.8	0.057	Not specific	
Combined	Gas7	growth arrest specific 7	−0.8	0.033	Yes	Yes
Array1	Esrrb	estrogen related receptor, beta	−0.8	0.089	PT	
Array1	Chrna4	cholinergic receptor, nicotinic, alpha polypeptide 4	−0.8	0.041	ET+PT	
Array1	Efna5	ephrin A5	−0.8	0.057	Yes 38/76 (50.0%)	Yes** 16/76 (21.1%)

Table II

Up-regulated genes due to the loss of *Gbx2*

key	Symbol	Description	logFC	adj.P.Val	Expression	Verified
Combined	Hist1h2ai	histone cluster 1, H2ai	0.8	0.049	NA	
Combined	Irx1	Iroquois related homeobox 1 (Drosophila)	0.8	0.008	Yes	Yes
Array1	Cenpe	centromere protein E	0.8	0.030	NA	
Array1	H2-D1	histocompatibility 2, D region locus 1	0.9	0.081	NA	
Array1	Hist2h2aa2	histone cluster 2, H2aa2	0.9	0.032	NA	
Combined	Kif4	kinesin family member 4	0.9	0.047	No expression	
Array1	Nrp2	neuropilin 2	0.9	0.069	Yes	Yes
Array1	Rad51ap1	RAD51 associated protein 1	0.9	0.089	No signals	
Array1	Enc1	ectodermal-neural cortex 1	0.9	0.053	Yes	
Array1	Hist1h2ah	histone cluster 1, H2ah	0.9	0.041	NA	
Combined	Dcx	doublecortin	0.9	0.033		
Combined	Fam111a	family with sequence similarity 111, member A	0.9	0.019	No expression	
Combined	Chd9	chromodomain helicase DNA binding protein 9	0.9	0.009	NA	
Array1	BC003331	cDNA sequence BC003331	1.0	0.023	NA	
Combined	Rrm1	ribonucleotide reductase M1	1.0	0.047	Yes?	
Combined	Kif26a	kinesin family member 26A	1.0	0.031	Yes	Yes
Array1	Hist1h2ak	histone cluster 1, H2ak	1.0	0.023	NA	
Combined	Fam65b	family with sequence similarity 65, member B	1.0	0.069	NA	
Combined	Otx1	orthodenticle homolog 1	1.0	0.004	PT	
Combined	Angpt1	angiopoietin 1	1.1	0.033	NA	
Combined	Smyd2	SET and MYND domain containing 2	1.1	0.005	Ubiquitous	
Array1	Ppp2r2b	protein phosphatase 2 (formerly 2A), regulatory subunit B (PR 52), beta isoform	1.1	0.025	Yes	
Combined	Tle4	transducin-like enhancer of split 4, homolog of Drosophila E(spl)	1.1	0.074	Yes	Yes
Combined	Thsd4	thrombospondin, type I, domain containing 4	1.1	0.019	No expression	
Combined	Rftn1	raftlin lipid raft linker 1	1.1	0.018	Yes	
Combined	Top2a	topoisomerase (DNA) II alpha	1.1	0.065	Not expressed	
Array1	Ccnd1	cyclin D1	1.2	0.075	Not expressed	
Array1	Col2a1	collagen, type II, alpha 1	1.2	0.028	Yes	
Combined	Arhgap12	Rho GTPase activating protein 12	1.2	0.044	Ubiquitous	
Combined	Epb4.1	erythrocyte protein band 4.1	1.3	0.073	NA	
Array1	Igfbpl1	insulin-like growth factor binding protein-like 1	1.4	0.015	both ET and Th	
Combined	Nefm	neurofilament, medium polypeptide	1.4	0.037	Yes	Yes
Combined	Shisa2	shisa homolog 2 (Xenopus laevis)	1.4	0.003	NA	
Combined	Fam196b	family with sequence similarity 196, member B	1.4	0.044	NA	
Combined	Mmd2	monocyte to macrophage differentiation-associated 2	1.4	0.037	Yes	
Array1	Map2	microtubule-associated protein 2	1.5	0.006	Ubiquitous	
Combined	Eml5	echinoderm microtubule associated protein like 5	1.6	0.053	NA	

key	Symbol	Description	logFC	adj.P.Val	Expression	Verified
Combined	Actb	actin, beta	1.6	0.068	NA	
Combined	Ebf3	early B cell factor 3	1.6	0.037	Yes	Yes
Combined	Cpne8	copine VIII	1.6	0.086	NA	
Combined	Olfm1	olfactomedin 1	1.8	0.038	Yes	
Combined	Ptx3	pentraxin related gene	1.8	0.077	NA	
Combined	Ephb1	Eph receptor B1	1.9	0.065	Yes	
Combined	Irx2	Iroquois related homeobox 2 (Drosophila)	2.0	0.069	Yes	Yes
Combined	Cntn2	contactin 2	2.1	0.038	Yes	Yes
Combined	Islr2	immunoglobulin superfamily containing leucine-rich repeat 2	2.2	0.037	Yes	Yes
Array1	Zic4	zinc finger protein of the cerebellum 4	2.3	0.017		NC
Combined	Lmo3	LIM domain only 3	2.8	0.020	Yes 18/48 (37.5%)	Yes 10/48 (20.8%)

Table III

Thalamus-enriched genes

Symbol	Description	logFC	adj.P.Val	Loss in Gbx2-KO
Gbx2	gastrulation brain homeobox 2	−6.16	8.85E-05	Yes
Sema5a	sema domain, seven thrombospondin repeats (type 1 and type 1-like), trans	−3.94	6.22E-05	
Chst1	carbohydrate (keratan sulfate Gal-6) sulfotransferase 1	−3.37	1.14E-03	Yes
Syt13	synaptotagmin XIII	−3.03	1.94E-03	Yes
Cyp1b1	cytochrome P450, family 1, subfamily b, polypeptide 1	−2.99	2.58E-04	Yes
Gng8	guanine nucleotide binding protein (G protein), gamma 8	−2.77	4.30E-03	
Crabp2	cellular retinoic acid binding protein II	−2.48	1.29E-03	
Nrn1	neuritin 1	−2.24	2.23E-02	
Id4	inhibitor of DNA binding 4	−2.00	2.58E-04	Yes
Hs6st2	heparan sulfate 6-O-sulfotransferase 2	−2.00	1.26E-02	Yes
Ntng1	netrin G1	−1.98	1.36E-02	Yes
Sertad4	SERTA domain containing 4	−1.84	8.95E-03	Yes
Robo2	roundabout homolog 2 (Drosophila)	−1.64	2.59E-02	Yes
Sorcs2	sortilin-related VPS10 domain containing receptor 2	−1.55	2.58E-04	
Gm10304	predicted gene 10304	−1.54	4.92E-02	Yes
Cd47	CD47 antigen (Rh-related antigen, integrin-associated signal transducer)	−1.53	2.38E-03	Yes
Rora	RAR-related orphan receptor alpha	−1.53	1.65E-02	Yes
Nr5a2	nuclear receptor subfamily 5, group A, member 2	−1.51	4.30E-03	
Prmt8	protein arginine N-methyltransferase 8	−1.43	2.07E-02	Yes
Osbpl3	oxysterol binding protein-like 3	−1.39	1.61E-03	
Hs3st1	heparan sulfate (glucosamine) 3-O-sulfotransferase 1	−1.31	4.30E-03	
Pou2f2	POU domain, class 2, transcription factor 2	−1.31	2.22E-02	
Ldb2	LIM domain binding 2	−1.31	4.29E-02	
Thsd7b	thrombospondin, type I, domain containing 7B	−1.28	1.39E-02	Yes
Sel1l3	sel-1 suppressor of lin-12-like 3 (C. elegans)	−1.21	2.85E-02	Yes
Arhgap18	Rho GTPase activating protein 18	−1.12	1.27E-02	
Tmtc2	transmembrane and tetratricopeptide repeat containing 2	−1.11	8.32E-03	
Tmem132a	transmembrane protein 132A	−1.09	3.48E-02	
Snx10	sorting nexin 10	−1.08	2.22E-02	
Lima1	LIM domain and actin binding 1	−1.07	3.00E-02	
1700025G04Rik	RIKEN cDNA 1700025G04 gene	−1.05	3.79E-03	
Sgk1	serum/glucocorticoid regulated kinase 1	−1.01	2.02E-02	Yes
AI504432	expressed sequence AI504432	−1.01	2.69E-02	
Fign	fidgetin	−1.01	1.08E-02	
Fam78b	family with sequence similarity 78, member B	−1.01	4.65E-03	
Lhx9	LIM homeobox protein 9	−3.94	2.24E-07	
Olig3	oligodendrocyte transcription factor 3	−3.32	1.04E-03	
Necab2	N-terminal EF-hand calcium binding protein 2	−1.82	1.10E-02	
Kirrel3	kin of IRRE like 3 (Drosophila)	−1.52	1.31E-02	Yes 17/39 (43.6%)